ISSN 0023-1584, Kinetics and Catalysis, 2011, Vol. 52, No. 3, pp. 459–466. © Pleiades Publishing, Ltd., 2011.
Original Russian Text © V. Yu. Gavrilov, E.A. Ustinov, 2011, published in Kinetika i Kataliz, 2011, Vol. 52, No. 3, pp. 470–477.

Dihydrogen Adsorption Isotherms (77 K) on Carbon Nanomaterials

V. Yu. Gavrilov[a] and E. A. Ustinov[b]

[a] *Boreskov Institute of Catalysis, Siberian Branch, Russian Academy of Sciences, Novosibirsk, 630090 Russia*
[b] *Ioffe Physicotechnical Institute, Russian Academy of Sciences, St. Petersburg, 194021 Russia*
e-mail: gavrilov@catalysis.ru

Received June 18, 2010

Abstract—Dihydrogen adsorption at 77 K on a number of fine-particle carbon materials, activated carbons, and carbon nanotubes has been investigated. The micropore structure parameters of these materials have been determined using a volumetric comparative method and nonlocal density functional theory (NLDFT). These data processing methods lead to different values of textural parameters. This difference is attributed to the presence of specific sorption sites on the surface of real carbon materials. The pore size range in which the NLDFT method is applicable to the C–H_2 system has been determined. A comparison between the hydrogen sorption properties of different carbon nanotubes is presented.

DOI: 10.1134/S0023158411030074

Sorption is among the basic experimental methods of characterization of the porous structure of nanomaterials, including heterogeneous catalysts [1]. Adsorption data processing has a long history; nevertheless, in recent years there is a tendency to their improvement and extension using precise molecular calculations, numerical Monte Carlo and molecular dynamics methods, and nonlocal density functional theory (NLDFT) [2–6]. At the same time, more conventional, continual techniques are not losing their attractiveness and remain widespread, largely because they are properly understood and simple to use.

Investigation of the microporous structure of carbon nanomaterials is an essential step in the synthesis of catalysts and adsorbents with preset textural properties for a wide variety of practical purposes, such as gas purification in industry and auto transport, hydrogen storage, and biological and medicinal applications [7]. Use of conventional nitrogen vapor adsorption (77 K) and argon vapor adsorption (87 K) techniques in micropore characterization relies on the possibility of the activated diffusion of adsorbed molecules in the ultrafine-pore space [8, 9]. A sharp decrease in the rate of reaching adsorption equilibrium leads to erroneous measurements. The problem of activated diffusion is solvable in two ways, namely, by using a sorbate with a smaller kinetic molecular size, such as dihydrogen (σ_k = 0.289 nm for H_2 against σ_k = 0.364 nm for N_2) [10, 11], and by conducting the sorption experiment at a higher temperature, for example, at 195 K with CO_2 as the sorbate [12]. This increases the kinetic energy of the sorbate molecules and facilitates diffusion in the ultrafine-pore space, but reduces the measurable equilibrium amount adsorbed.

One way of processing isotherms of hydrogen physisorption on microporous solids is by employing the continual volumetric comparative method [13], which enables one to estimate the volume of the micropores accessible to sorbate molecules. This method uses independent data on the amount of hydrogen adsorbed per unit area of mesopores differing in their chemical nature ($\alpha(P)$) and the density of the sorbate in a unit volume of micropores ($\beta(P)$), where P is the equilibrium sorbate pressure. Obtaining these relationships is a separate and rather complicated problem involving selection of disperse samples whose surface is chemically identical or at least similar to the surface of the wide class of materials to be examined. The $\alpha(P)$ values for oxide materials, obtained in an earlier study [14], were used in an analysis of experimental hydrogen adsorption isotherms for ultrafine MCM-41 samples, zeolite ZSM-5, and their mechanical mixtures [13]. Note that the similarity between the sorption processes on the materials to be examined and the same processes on the selected reference materials is verified by checking the affinity of adsorption isotherms, which can be evaluated in terms of the linear correlation coefficient.

The purpose of this work is to extend the range of applicability of H_2 physisorption at 77 K to characterization of ultrafine carbon materials by calculating their textural parameters by the comparative and NLDFT methods.

EXPERIMENTAL

The objects of our study were structurally diverse, differently synthesized microporous carbon nanomaterials (CNMs), activated carbons, and high-porosity carbon nanotubes (CNTs).

Hydrogen and nitrogen adsorption isotherms for carbon materials at 77 K in a wide pressure range (2×10^{-5}–1 atm) were measured using a DigiSorb 2600 Micromeritics automated volumetric instrument (United States). All samples were conditioned in vacuo at 350°C and a residual pressure of 10^{-4} Torr for 5 h.

Carbon nanotubes were examined under a JEM 2010 electron microscope (Japan) with a resolution of 1.4 Å at an accelerating voltage of 200 kV.

RESULTS AND DISCUSSION

The basic relationship of the volumetric comparative method is the following expression for the hydrogen adsorption isotherm [14]:

$$A(P) = A^0 + S_\alpha \alpha(P) + V_\mu \beta(P), \quad (1)$$

where A^0 is the total value of specific adsorption (e.g., on Lewis and the other possible surface sites [15]), S_α is the surface area of the mesopores and macropores, $\alpha(P)$ is the amount of hydrogen adsorbed by a unit area of the mesopores and macropores, V_μ is the micropore volume, $\beta(P)$ is the amount of hydrogen sorbed by a unit volume of the micropores. It follows from Eq. (1) that the amount adsorbed $A(P)$ is a function of two independent variables, namely, $\alpha(P)$ and $\beta(P)$, which can reliably be determined experimentally.

For carbon surfaces, $\alpha(P)$ can be derived from results obtained for mesoporous/macroporous pyrolysis carbon blacks. However, gaining these data involves experimental difficulties arising from the small specific surface area of the carbon blacks and from the small amount of hydrogen adsorbed per unit area of the mesopores at 77 K. These circumstances can cause unacceptably large experimental errors, particularly at low sorbate pressures. It is these circumstances that did not allow the absolute amounts of H_2 adsorbed on pyrolysis carbon black at $P < 5$ Torr to be measured reliably in an earlier study [16]. The function $\beta(P)$ depends primarily on the sensitivity of the sorbate density in the micropores on the micropore structure.

The NLDFT analysis of adsorption isotherms aimed at determining the pore size distribution reduces to solving the Fredholm equation, which represents the excess adsorption isotherm $A(P)$ as follows [2]:

$$A(P) = \int [\rho(P, H) - \rho_b(P)] f(H) dH, \quad (2)$$

where $\rho(P, H)$ is the density of the sorbed phase in a pore with the width H at the pressure P, $\rho_b(P)$ is the density of the adsorptive at the pressure P, and $f(H)$ is the pore size distribution function. In practice, integral (2) is replaced with a sum of increments and the problem reduces to solving a set of linear algebraic equations for volume increments. The $f(H)$ function is determined by minimizing the sum of squared deviations between the experimental and calculated amounts adsorbed [17] under the constraint that the distribution function is nonnegative. The effect of random errors in measurements is reduced by using Tikhonov's regularization (smoothing) method [18].

The NLDFT analysis of the microporous structure of carbon materials was carried out using the 77-K H_2 adsorption isotherm for graphitized carbon black as the reference system, for which the following parameters of the Lennard-Jones (12-6) potential were accepted by Jagiello et al. [19]: for the interaction between sorbate molecules, a collision diameter of $\sigma_{ff} = 0.304$ nm and a binary interaction parameter of $\varepsilon_{ff}/k = 34.3$ K; for the C–H_2 interaction, $\sigma_{sf} = 0.322$ nm and $\varepsilon_{sf}/k = 31.8$ K. However, there is good reason to believe that the collision diameter σ_{ff} accepted by Jagiello et al. [19] is somewhat overestimated. More accurate values of the molecular parameters can be derived from PVT tables [20] using the equation of state that follows from NLDFT for a homogeneous gas [21, 22]. In this case, accepting that the equivalent diameter of a hard sphere (d_{HS}) is equal to the collision diameter σ_{ff}, we obtain $\sigma_{ff} = 0.2893$ nm and $\varepsilon_{ff}/k = 28.20$ K. The C–H_2 interaction parameters can now be derived from the hydrogen adsorption isotherm corresponding to the parameters accepted by Jagiello et al. [19]: $\sigma_{sf} = 0.3146$ nm and $\varepsilon_{sf}/k = 33.93$ K. In our calculations, we also took into account the Feynman quantum correction to the hydrogen–graphitized carbon black interaction potential [23].

Using the parameters thus determined, we calculated a series of local hydrogen adsorption isotherms, $\rho(P, H)$, for slitlike model pores with a width of $H = 0.55$–10 nm for a pressure range of $P = 10^{-5}$–1 atm. Some of these isotherms are plotted in Fig. 1. The dashed line represents the hydrogen adsorption isotherm for a micropore 0.6 nm in width. The other lines but the last were obtained for pores whose width changes between 0.7 and 1.5 nm from left to right with 0.1-nm increments. The last isotherm refers to a 2-nm-wide pore. It is clear from Fig. 1 that, in the micropores narrower than 0.7 nm, a decrease in the pore width shifts the isotherm to higher pressures. This is due to the superposition of the potentials of hydrogen repulsion from the opposite walls.

Figure 2 shows the calculated excess amount of hydrogen adsorbed in the slitlike model pores versus pore width at fixed pressures of 0.1 to 1 atm (sorption isobars). The amounts of hydrogen adsorbed refer to a unit area of one of the pore walls. It can be seen from Fig. 2 that H_2 adsorption takes place in micropores whose width is above 0.55 nm. An increase in the distance between the pore walls causes a weakening of the

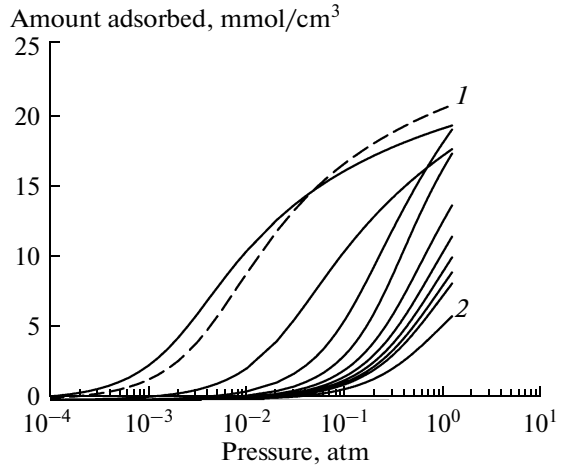

Fig. 1. Calculated isotherms of H_2 adsorption in slitlike pores at 77 K. Pore width: (*1*) 0.6 and (*2*) 2.0 nm. For the other curves from left to right, the pore width increases from 0.7 to 1.5 nm with 0.1 nm increments.

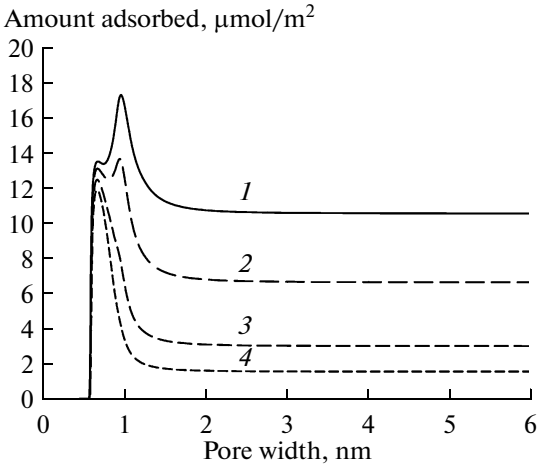

Fig. 2. Calculated excess amount of H_2 adsorbed in slitlike pores as a function of the pore width for $T = 77$ K and $P =$ (*1*) 1, (*2*) 0.5, (*3*) 0.2, and (*4*) 0.1 atm.

repulsive forces and leads to the domination of the attractive forces, which are strengthened by the superposition of the potentials due the opposite walls of the micropore. As a consequence, the amount adsorbed increases and passes through a maximum at a pore width of about 1 nm for $P = 1$ atm and 0.665 nm for $P = 0.1$ atm. A further increase in the micropore width reduces the opposite wall potential superposition effect and, accordingly, causes a decrease in the amount adsorbed. Starting at $H = 2$ nm, the pore width has no effect on the amount of H_2 adsorbed because hydrogen adsorption on the opposite walls of the micropore occurs independently, as in the case of macroporous graphitized carbon black. The ultimate amount of hydrogen adsorbed in the micropores wider than 2 nm is exactly equal to the doubled amount of hydrogen adsorbed on the carbon black surface. Therefore, from a hydrogen adsorption isotherm measured in a pressure range below 1 atm, one can derive only the micropore volume distribution over pore size (H). Below 0.1 atm, the amount of hydrogen adsorbed is insensitive to the pore size when the latter exceeds 1.5 nm (Fig. 2). Hence, the higher the sorbate pressure, the stronger the effect of wider pores on hydrogen adsorption. Therefore, in order to extend the pore range to mesopores using H_2 adsorption, it is necessary to raise the sorbate pressure substantially, probably up to several hundreds of atmospheres. At the same time, the smallest size (width in the slitlike pore model) of the pores accessible to hydrogen molecules in carbon materials is estimated at ~0.55 nm. This value is suggested by the position of the zero sorption potential point in the C–H_2 system, which corresponds to a distance of $0.85\sigma_{sf}$ from the pore wall. Accordingly, the smallest width of a pore accessible to hydrogen molecules is twice as large. Since the gas pressure in the sorptometer used in this study cannot be elevated above atmospheric pressure, this technique allows only the micropore size distribution and the total mesopore surface area (S_{meso}) to be determined reliably. The latter quantity is very sensitive to experimental errors; nevertheless, it can provide useful and suffi-

Table 1. Textural parameters of carbon nanomaterials derived from N_2 adsorption isotherms (77 K)

Material	S_α, m^2/g	$V\mu$, cm^3/g	V_s, cm^3/g
CNM-1	380	0.328	–
CNM-2	2650	0.105	2.13
CNM-3	223	0.159	0.33
Activated carbon SKT	181	0.367	0.525
Activated carbon SKN	587	0.337	1.063
Activated carbon Chemviron	251	0.394	0.564
Activated carbon SuperSorbon	501	0.266	0.542
Activated carbon Shell	153	0.366	0.449
CNT-1	870	0.021	1.92
CNT-2	180	0.018	2.21

Note: S_α = mesopore surface area, V_μ = micropore volume, and V_s = total pore volume.

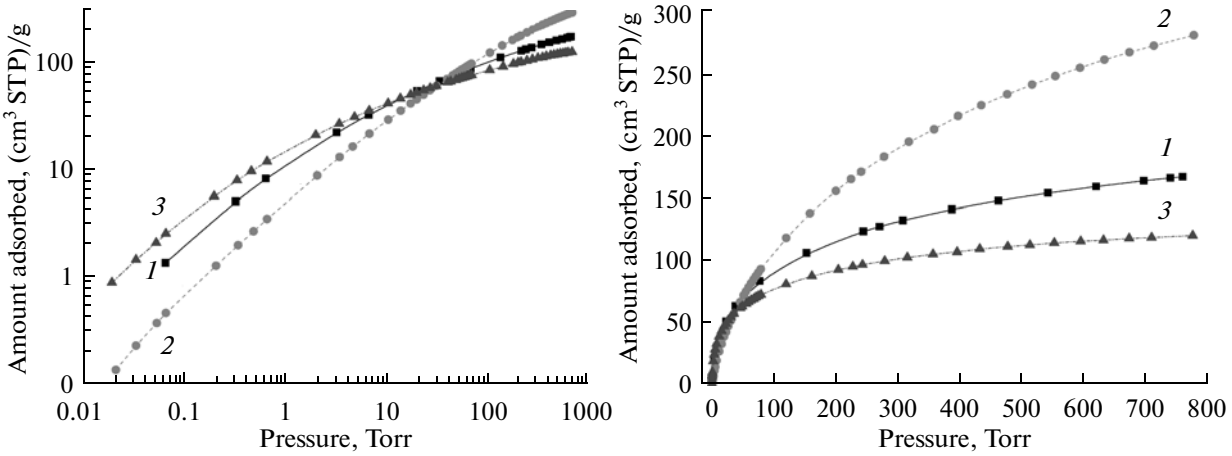

Fig. 3. H_2 adsorption isotherms (77 K) in logarithmic and linear forms for carbon nanomaterials: (*1*) CNM-1, (*2*) CNM-2, and (*3*) CNM-3.

ciently reliable information when used in combination with other calculated data.

Table 1 lists the textural characteristics calculated for the carbon nanomaterials by the conventional comparative method from N_2 adsorption isotherms (77 K) [24]. Clearly, the microporous samples examined vary widely in pore structure parameters. Figures 3–5 show typical H_2 adsorption isotherms (77 K) in logarithmic and linear forms measured for the same samples in a wide H_2 pressure range.

In Table 2, we compare the basic microporous structure parameters derived from H_2 adsorption isotherms by the comparative method to those calculated using NLDFT. The micropore volumes (V_μ, cm^3/g) determined by these methods are different and generally do not coincide with those determined via N_2 adsorption.

Table 2. Textural parameters of carbon nanomaterials derived from H_2 adsorption isotherms (77 K)

Material	Comparative method		NLDFT method		
	V_μ, cm^3/g	A^0, $(cm^3$ STP$)/g$	V_μ, cm^3/g	S_μ, m^2/g	S_{meso}, m^2/g
CNM-1	0.249	13.6	0.324	830	302
CNM-2	NA	NA	0.853	1736	7
CNM-3	0.154	28.2	0.284	739	0
Activated carbon SKT	0.317	23.2	0.463	1162	10
Activated carbon SKN	0.234	10.4	0.337	849	339
Activated carbon Chemviron	0.288	17.6	0.448	1092	0
Activated carbon SuperSorbon	0.170	10.4	0.365	848	0
Activated carbon Shell	0.267	26.4	0.396	1011	28
CNT-1	NA	NA	0.137	329	280
CNT-2	NA	NA	0.034	73	80

Note: V_μ = micropore volume, A^0 = specific adsorption value, S_μ = micropore surface area for the slitlike pore model, S_{meso} = mesopore surface area, and NA = nonaffine.

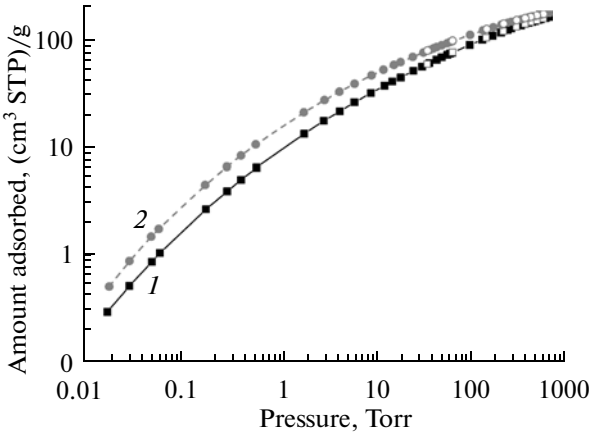

Fig. 4. H_2 adsorption isotherms (77 K) in logarithmic form for activated carbons: (*1*) SKN and (*2*) SKT.

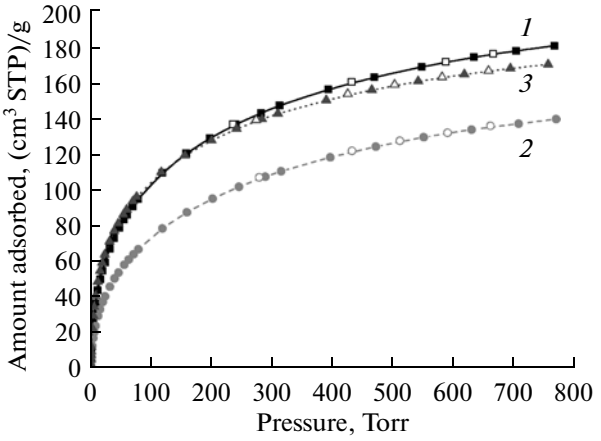

Fig. 5. H_2 adsorption isotherms (77 K) for activated carbons: (*1*) Chemviron, (*2*) SuperSorbon, and (*3*) Shell.

The microporous structure calculations from nitrogen and hydrogen adsorption isotherms by the comparative method are based on similar postulates stating the additivity of adsorption in the micropore space and on the mesopore surface. It is, therefore, likely that the difference between the $V_\mu^{N_2}$ and $V_\mu^{H_2}$ values is due to the different behaviors of the sorbate molecules in the micropores. It was demonstrated earlier [25] that the upper limit of the size of micropores (zone of an increased dispersion potential) depends on the size of the sorbate molecule, and this is in agreement with the data calculated using NLDFT. For nitrogen, whose molecules are larger, the volume of micropores with an increased adsorption potential is somewhat larger.

The micropore volumes derived from H_2 adsorption isotherms using NLDFT are larger than the V_μ values calculated by the comparative method. This is apparently due to the difference between the main approaches used in these techniques.

As was noted above, local adsorption isotherms are calculated for uniform homogeneous, or homotattic, surfaces [26]. Specific adsorption surface sites and various functional groups (characterized by their own intermolecular interaction constants with respect to the sorbate), which are undoubtedly present at large concentrations on the surface of real carbons [27], can cause some data distortion. Hydrogen adsorption is more sensitive to the presence of such sites than, e.g., nitrogen or argon adsorption. Based on adsorption data alone, it is impossible to estimate how significant

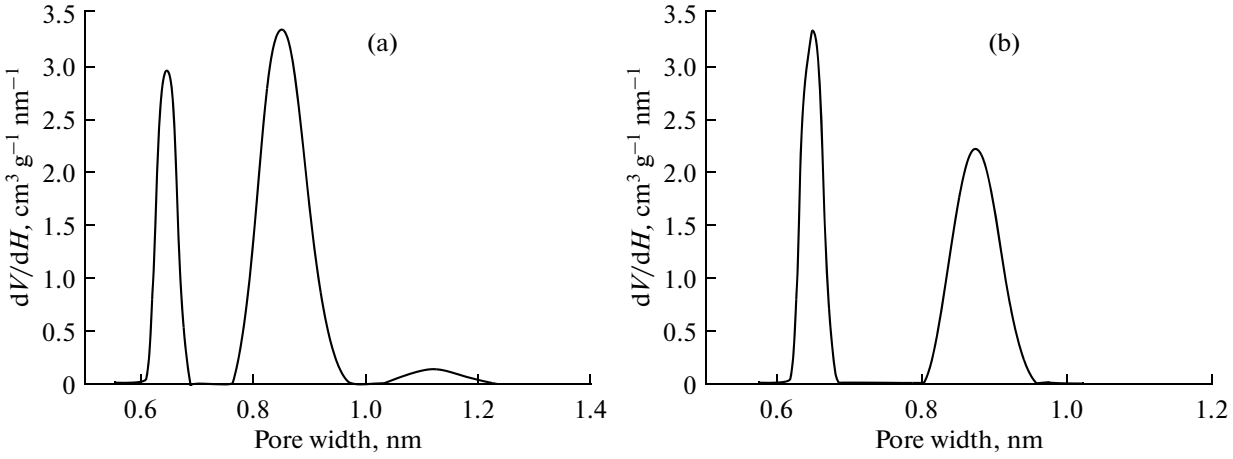

Fig. 6. Micropore size distribution calculated from the H_2 adsorption isotherm by the NLDFT method for (a) activated carbon SKT and (b) CNM-3.

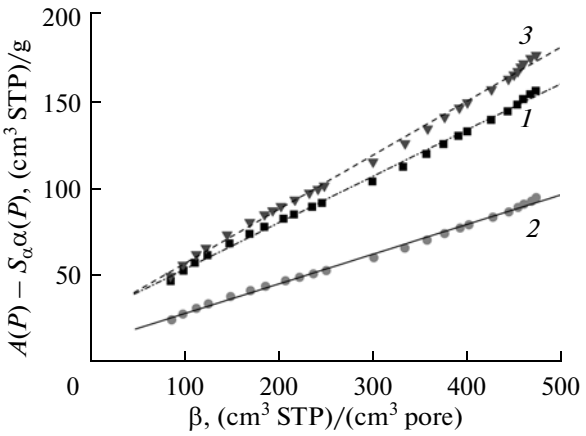

Fig. 7. Comparison plots of H_2 adsorption isotherms (77 K) for activated carbons: (*1*) Shell, (*2*) SuperSorbon, and (*3*) SKT.

these distortions are for the final result of isotherm analysis. At the same time, the comparative method enables one to reveal and separate the contribution from specific sorption aversus the reference data (A^0, Table 2). Thus, in the comparative method using Eq. (1), a considerable part of the adsorbed hydrogen is correlated not with the microtexture parameters, but with the chemical composition of the surface. It is likely this circumstance that is mainly responsible for the discrepancy between the V_μ values determined by the comparative and NLDFT methods.

The mesopore/macropore surface area (S_{meso}) values presented in Table 2, determined from hydrogen sorption data, cannot be considered as an alternative to the S_α values (Table 1) derived from nitrogen vapor adsorption data. The uncertainty in S_{meso} estimation far exceeds the errors in the conventional mesopore/macropore surface area measurements using nitrogen or argon vapor. This is due to the fact that the amount of H_2 adsorbed per unit area of the pore surface at 77 K is much smaller than the amount of N_2 or Ar adsorbed under the same conditions.

Figure 6a plots the pore size distribution $f(H)$ for activated carbon SKT calculated by the NLDFT method from H_2 adsorption isotherms for the slitlike pore model. This computational method demonstrated that this activated carbon has pores 0.6 to 1.2 nm in width with bimodal size distribution and dominant sizes of 0.65 and 0.85 nm. A plausible explanation of this fact is that graphene sheets are removed discretely as the carbon material is activated. Similarly shaped distribution curves were obtained for other activated carbon samples. The micropore size distribution for CNM-3 (Fig. 6b) is also bimodal, with

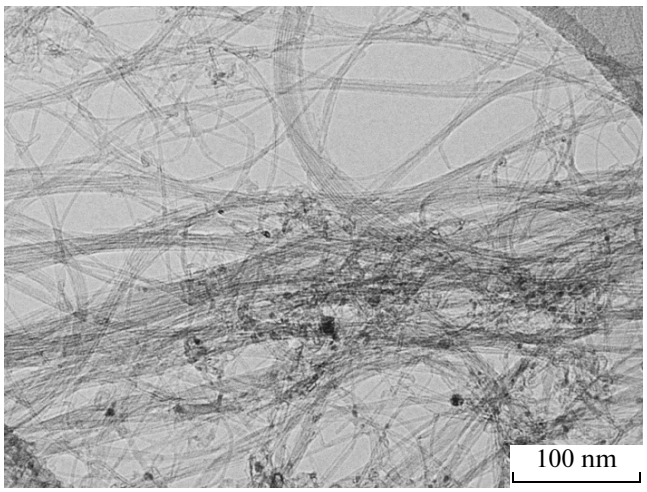

Fig. 8. Micrograph of the CNT-1 thin-wall nanotubes.

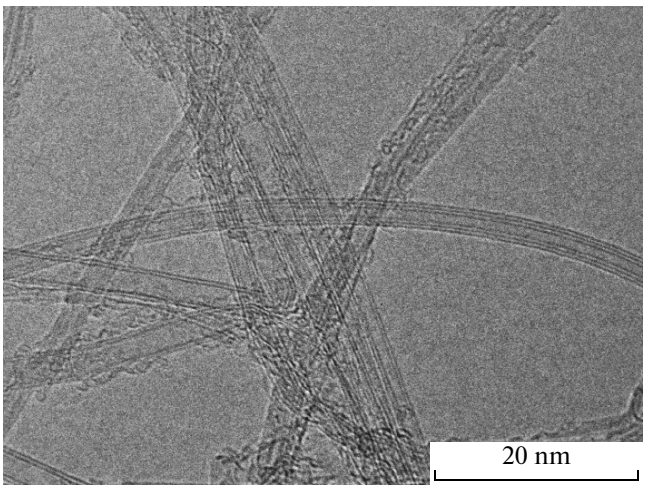

Fig. 9. High-resolution micrograph of CNT-1.

dominant pore sizes of 0.65 and 0.87 nm. Apparently, this kind of pore size distribution is typical for CNMs as well.

Processing of H_2 adsorption data by the comparative method demonstrates that the adsorption isotherms for most samples are affine, with a linear correlation coefficient of ~0.998 (Fig. 7). The exceptions are CNT-1 and CNM-2. For these materials, the comparison plot deviates from linearity, and this does not allow the micropore volume to be correctly estimated by the comparative method (see NA in Table 2). The difference between the sorption properties of these sample and those of the other carbon materials can be due to the specific features of their surface composition and porous structure. For single-wall nanotubes, these specific features of sorption were considered by Eletskii [28].

Figure 8 shows a micrograph of the CNT-1 sample. Morphologically, CNT-1 is an extremely loose packing of nanotubes aggregated in bundles, each containing several tens of nanotubes. Single nanotubes are also observed. Along with the nanotube packings, there are particles of amorphous carbon (20–30 nm and larger) and graphite with an imperfect structure (interplanar spacing of $d \sim 0.354$ nm). There are also minor quantities of round particles of a metal, whose size is about 5 nm, which are likely traces of the catalyst used in the synthesis. Figure 9 shows a high-resolution micrograph of CNT-1, from which it is clear that the walls of the nanotubes consist mostly of two or three graphene sheets. The outer diameter of a nanotube is 2.6–2.8 nm, and the inner diameter of the channel is 1.5–2 nm. It is possible that the thin wall, a few graphene sheets thick, is among the factors determining the sorption properties of the nanotube. Another factor can be the above-mentioned presence of amorphous carbon, whose sorption properties [29], including the energy of interaction with hydrogen, differ from those of, e.g., single-wall nanotubes.

In order to verify this assumption, we studied hydrogen adsorption on thicker wall nanotubes (CNT-2), whose micrograph is shown in Fig. 10 [30]. The wall of a nanotube consists of more than ten graphene sheets. According to nitrogen adsorption data, the accessible surface area of CNT-2 is appreciably smaller than that of the thin-wall nanotube CNT-1. The micrograph indicates the presence of closed-end nanotubes. Kuznetsov et al. [30] noted that this nanotube sample is practically free of amorphous carbon and metallic components of the catalyst. At the same time, an analysis of the H_2 adsorption isotherm by the comparative method indicates insufficient affinity (NA in Table 2).

Figure 11 presents a comparison between the H_2 adsorption isotherms of CNT-1 and CNT-2, both in terms of the amount adsorbed per unit area of the accessible surface, S_α. The isotherms differ significantly in shape, and CNT-2 adsorbs less hydrogen than CNT-1. This difference between the adsorption properties of the nanotube samples may be evidence of the effects of the carbon wall thickness and the impurities present in CNT-1. It is impossible to see which of the factors is dominant. Nevertheless, the comparative analysis of hydrogen adsorption isotherms makes it possible to reveal the difference between the adsorption properties of different types of carbon materials.

Thus, the results of this study suggest that the analysis of hydrogen adsorption isotherms (77 K) using the volumetric comparative method and NLDFT provides means to reliably calculate microtexture parameters in the framework of the postulates underlying these methods. However, it is necessary to take into account the above-noted specific features of applying these

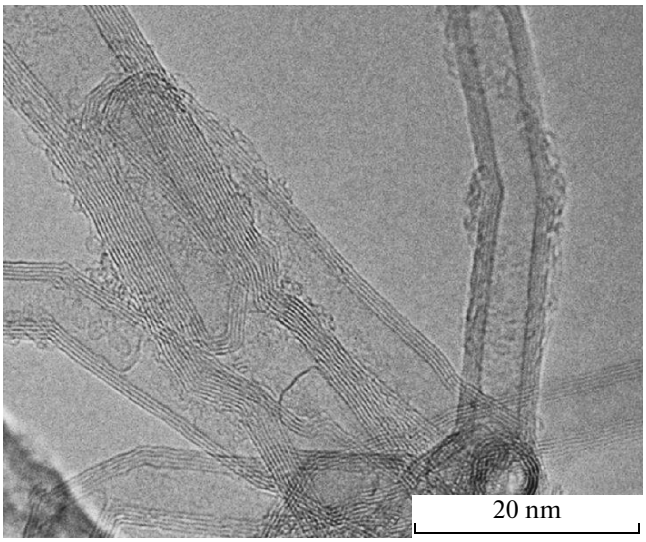

Fig. 10. High-resolution micrograph of the CNT-2 thick-wall nanotubes [30].

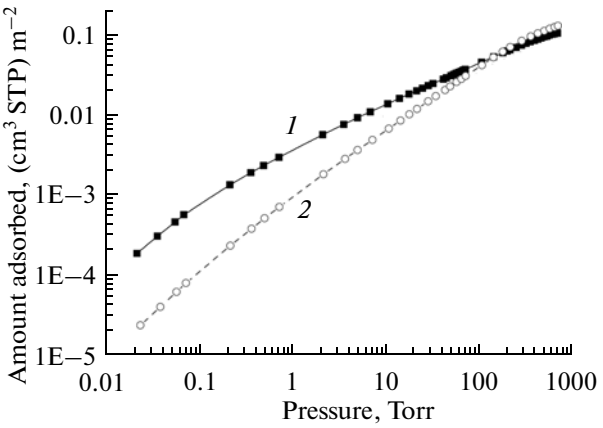

Fig. 11. H_2 adsorption isotherms (77 K) for (*1*) CNT-1 and (*2*) CNT-2.

methods to real carbon materials and those of comparing the results.

ACKNOWLEDGMENTS

The authors are grateful to V.L. Kuznetsov for providing carbon nanotubes and to A.V. Ishchenko for electron microscopic examinations. E.A. Ustinov acknowledges support from the Russian Foundation for Basic Research (project no. 09-03-12153-OFI-m).

REFERENCES

1. Rouquerol, F., Rouquerol, J., and Sing, K.S.W., *Adsorption by Powders and Porous Solids: Principles, Methodology and Applications*, London: Academic, 1999, p. 467.
2. Maddox, M.W., Olivier, J.P., and Gubbins, K.E., *Langmuir*, 1997, vol. 13, p. 1737.
3. Lastoskie, Ch.M. and Gubbins, K.E., *Stud. Surf. Sci. Catal.*, 2000, vol. 128, p. 41.
4. Ustinov, E.A. and Do, D.D., *Langmuir*, 2004, vol. 20, p. 3791.
5. Ustinov, E.A., Do, D.D., and Fenelonov, V.B., *Carbon*, 2006, vol. 44, p. 653.
6. Neimark, A.V., Lin, Y., Ravikovitch, P.I., and Thommes, M., *Carbon*, 2009, vol. 47, p. 1617.
7. Fenelonov, V.B., *Poristyi uglerod* (Porous Carbon), Novosibirsk: Inst. Kataliza, 1995.
8. Sweatman, M.B. and Quirke, N., *J. Phys. Chem. B*, 2001, vol. 105, p. 1403.
9. Jagiello, J. and Thommes, M., *Carbon*, 2004, vol. 42, p. 1227.
10. Gavrilov, V.Yu., *Kinet. Katal.*, 1995, vol. 36, no. 4, p. 631.
11. Jagiello, J. and Bets, W., *Microporous Mesoporous Mater.*, 2008, vol. 108, p. 117.
12. Gavrilov, V.Yu. and Zakharov, R.S., *Kinet. Katal.*, 2010, vol. 51, no. 4, p. 633 [*Kinet. Catal.* (Engl. Transl.), vol. 51, no. 4. p. 609].
13. Gavrilov, V.Yu., *Kinet. Katal.*, 2007, vol. 48, no. 6, p. 856 [*Kinet. Catal.* (Engl. Transl.), vol. 48, no. 6, p. 799].
14. Gavrilov, V.Yu., *Kinet. Katal.*, 2005, vol. 46, no. 4, p. 642 [*Kinet. Catal.* (Engl. Transl.), vol. 46, no. 4, p. 603].
15. Kazansky, V.B., *J. Catal.*, 2003, vol. 216, nos. 1–2, p. 192.
16. Gavrilov, V.Yu., *Kinet. Katal.*, 1995, vol. 36, no. 5, p. 787.
17. Ustinov, E.A., Fenelonov, V.B., Yakovlev, V.A., and Eletskii, P.I., *Kinet. Katal.*, 2007, vol. 48, no. 4, p. 629 [*Kinet. Catal.* (Engl. Transl.), vol. 48, no. 4, p. 589].
18. Tikhonov, A.N. and Arsenin, V.Y., *Solution of Ill-Posed Problems*, New York: Wiley, 1977.
19. Jagiello, J., Anson, A., and Martinez, M.T., *J. Phys. Chem. B*, 2006, vol. 110, p. 4531.
20. Vargaftik, N.B., *Spravochnik po teplofizicheskim svoistvam gazov i zhidkostei* (A Handbook of Thermal and Physical Properties of Gases and Liquids), Moscow: Nauka, 1972.
21. Tarazona, P., *Phys. Rev. A: At. Mol. Opt. Phys.*, 1985, vol. 31, p. 2672.
22. Tarazona, P., Marconi, U.M.B., and Evans, R., *Mol. Phys.*, 1987, vol. 60, p. 573.
23. Stan, G. and Cole, M.W., *J. Low Temp. Phys.*, 1998, vol. 110, nos. 1–2, p. 539.
24. Karnaukhov, A.P., *Adsorbtsiya. Tekstura dispersnykh i poristykh materialov* (Adsorption: Texture of Disperse and Porous Materials), Novosibirsk: Nauka, 1999.
25. Everett, D.H. and Powl, J.C., *J. Chem. Soc., Faraday Trans. 1*, 1976, vol. 72, p. 619.
26. Ustinov, E.A., *Langmuir*, 2009, vol. 25, no. 13, p. 7450.
27. Jaycock, M.J. and Parfitt, G.D., *Chemistry of Interfaces*, New York: Ellis Horwood, 1981.
28. Eletskii, A.V., *Usp. Fiz. Nauk*, 2004, vol. 174, no. 11, p. 1191.
29. Dillon, A.C., Jones, K.M., Bekkedahl, T.A., Kiang, C.H., Bethune, D.S., and Heben, M.J., *Nature*, 1997, vol. 386, p. 377.
30. Kuznetsov, V.L., Elumeeva, K.V., Ischenko, A.V., Beylina, N.Yu., Stepashkin, A.A., Moseenkov, S.I., Plyasova, L.M., Molina, I.Yu., Romanenko, A.I., Anikeeva, O.B., and Tkachev, E.N., *Phys. Status Solidi B*, 2010, vol. 247, nos. 11–12, p. 2695.